



저작자표시-비영리-동일조건변경허락 2.0 대한민국

이용자는 아래의 조건을 따르는 경우에 한하여 자유롭게

- 이 저작물을 복제, 배포, 전송, 전시, 공연 및 방송할 수 있습니다.
- 이차적 저작물을 작성할 수 있습니다.

다음과 같은 조건을 따라야 합니다:



저작자표시. 귀하는 원저작자를 표시하여야 합니다.



비영리. 귀하는 이 저작물을 영리 목적으로 이용할 수 없습니다.



동일조건변경허락. 귀하가 이 저작물을 개작, 변형 또는 가공했을 경우에는, 이 저작물과 동일한 이용허락조건하에서만 배포할 수 있습니다.

- 귀하는, 이 저작물의 재이용이나 배포의 경우, 이 저작물에 적용된 이용허락조건을 명확하게 나타내어야 합니다.
- 저작권자로부터 별도의 허가를 받으면 이러한 조건들은 적용되지 않습니다.

저작권법에 따른 이용자의 권리는 위의 내용에 의하여 영향을 받지 않습니다.

이것은 [이용허락규약\(Legal Code\)](#)을 이해하기 쉽게 요약한 것입니다.

[Disclaimer](#)

공학석사학위논문

Screening Method of Tyrosinase with  
Higher Ratio of Monophenolase/Diphenolase  
Activity for Phenolic Natural Compounds

2014년 2월

서울대학교 대학원

화학생물공학부

백기헌

Screening Method of Tyrosinase with  
Higher Ratio of Monophenolase/Diphenolase  
Activity for Phenolic Natural Compounds

By Kiheon Baek

Advisor: Professor Byung-Gee Kim, Ph.D.

Submitted in partial fulfillment of the requirement  
for the Master of Science in Engineering degree

February, 2014

School of Chemical and Biological Engineering  
Seoul National University

Screening Method of Tyrosinase with Higher  
Ratio of Monophenolase/Diphenolase Activity for  
Phenolic Natural Compounds

자연계 페놀류 물질에 대한 상향된 모노페놀레이즈/  
다이페놀레이즈 비율의 티로시나아제를 스크리닝하는 방법에  
대한 고찰

지도교수 김병기

이 논문을 공학석사학위논문으로 제출함

2014년 2월

서울대학교 대학원

화학생명공학부

백기현

백기현의 공학석사 학위논문을 인준함

2014년 2월

위원장 \_\_\_\_\_ (인)

부위원장 \_\_\_\_\_ (인)

위원 \_\_\_\_\_ (인)

## Abstract

*ortho*-Monohydroxylation of daidzein, resveratrol and apigenin was attempted using tyrosinase. Tyrosinase proceeds two consecutive oxidation reactions, hydroxylation of monophenol compounds to diphenolic compounds (monophenolase reaction) and successive oxidation to make quinonic compounds (diphenolase reaction). Since the second step oxidation reaction consumes the first step diphenolic products such as piceatannol, 7,3',4'-trihydroxyisoflavone (3'-ODI), and tricetin, the yield of the first step products is quite low, limiting the use of tyrosinase for such monohydroxylation reaction. To overcome the drawback of tyrosinase, the changes in the ratio of monophenolase activity ( $k_1$ ) to diphenolase activity ( $k_2$ ) were attempted.

For changing the ratio of monophenolase activity to diphenolase activity, our group developed a screening method and a method for obtaining kinetic constants and did a site-saturation mutagenesis with a tyrosinase from *Streptomyces avermitilis* MA4680 (SAV1137). According to the result, one mutant having higher ratio (1.4 fold higher than wild type) and productivity of piceatannol (1.4 fold higher than wild type) was found. However, the process was pretty labor-intensive, and the accuracy was poor. 5 mutants were screened from 300 mutants, but the only one mutants had meaningful value. Therefore, accuracy-improved and unexacting screening method was required.

By changing pH and strength of buffer, concentration of iron and cell extract solution, and addition of 3-methyl-2-benzothiazolinone hydrazone hydrochloride (MBTH), we developed improved screening method which traces an accumulative quantity of diphenolic compounds in real time with UV spectrometer and an improved assay method for obtaining kinetic constants of mutants.

For testifying screening method and finding mutants having higher ratio for natural phenolic compounds, site-saturation mutagenesis of tyrosinase from *Bacillus megaterium* was performed using the screening method based on x-ray crystal structure, homology modeling and enzyme-substrate docking simulation. Single mutations at V218S was effective to increase the yield of 3'-ODI by 30% than by wild type and the yield of piceatannol by V218G was increased 440% than by wild type. R209A was also effective to increase the yield of tricetin by 40% comparing with wild type. Among these mutations, V218S showed 10.7 fold ratio change of  $k_1$  to  $k_2$  for daidzein and V218G showed 1.4 fold ratio change of  $k_1$  to  $k_2$  for resveratrol.

**Key words** : tyrosinase, screening, *Bacillus megaterium*, iron chelation, daidzein, resveratrol

**Student number** : 2012-20950

# Contents

Abstract .....	1
Contents .....	3
List of Tables .....	5
List of Figures .....	6
Abbreviations .....	7
1. Introduction .....	8
2. Materials and Methods .....	12
2.1. Plasmids construction for recombinant tyrosinase and variants by mutagenesis .....	12
2.2. Expression of recombinant tyrosinase and variants for screening .....	14
2.3. Screening method for substrates .....	15
2.4. Purification of tyrosinase .....	15
2.5. Characterization of tyrosinase .....	16
2.6. Oxidative reaction with substrates .....	16
2.7. Analytical methods .....	17

3. Results and Discussion .....	18
3.1. Developing a screening method with substrates .....	18
3.2. Selecting residues for mutagenesis and screening for high yield of substrates	25
3.3. Identification of products from each substrate .....	32
3.4. Developing a method for measuring kinetic constants .....	37
3.5. Characterization of mutants and interpretation with modeling and docking	40
4. Conclusion .....	45
Reference .....	46
국문 초록 .....	49



# List of Tables

**Table 1.** Primer list

**Table 2.** Kinetic constants of wild type, V218S, and V218G with phenolic natural compounds.

## List of Figures

- Figure 1.** Absorbance at 550 nm of reaction with various conditions for testing screening method. ((a) ~ (c)) Relation between a concentration of diphenolic compounds and an absorbance. (d)
- Figure 2.** Strategy of screening method based on the cycle of tyrosinase.
- Figure 3.** Result of screening by phenolic natural compounds with libraries.
- Figure 4.** Products concentration of reaction with tyrosinase.
- Figure 5.** Representative GC/MS and GC/MS/MS electron impact mass spectra of TMS derivatives of products.
- Figure 6.** HPLC data of product from apigenin and quercetin.
- Figure 7.** The scheme for obtaining kinetic constants of tyrosinase with phenolic natural compounds.
- Figure 8.** Crystal structure and homology models of tyrosinase and mutants.

## Abbreviations

3'-ODI : 7,3',4'-trihydroxyisoflavone

MBTH : 3-methyl-2-benzothiazolinone hydrazone hydrochloride

L-DOPA : L-3,4-dihydroxyphenylalanine

LB : Luria-Bertani media

IPTG : Isopropyl  $\beta$ -D-1-thiogalactopyranoside

OD : Optical density

HPLC : High-performance liquid chromatography

TMS : trimethylsilyl

BSTFA : N,O-bis(trimethylsilyl)trifluoroacetamide

# 1. Introduction

Tyrosinase uses molecular oxygen to catalyze two consecutive oxidation reactions to phenol moiety of L-tyrosine; 1) monophenolase reaction: the *ortho*-hydroxylation of monophenols to *o*-diphenols and 2) diphenolase reaction: the oxidation of *o*-diphenols to *o*-quinones [1]. Since tyrosinase accepts not only L-tyrosine but also other mono-phenolic natural compounds as substrates, it has a great potential for the production of aromatic *ortho*-diol compounds beside phenol waste treatment [2].

However, since most of the previous studies of tyrosinase were performed mainly with L-tyrosine and L-3,4-dihydroxyphenylalanine (L-DOPA) as a model system, its accurate substrate specificity for other phenolic compounds was not well investigated and documented. According to the previous study done in our group [3], in the presence of catechol inhibitor, tyrosinase from *Streptomyces avermitilis* can do regiospecific *ortho*-hydroxylation of trans-resveratrol yielding piceatannol, which is known for potent inducer of apoptosis in the lymphoma cell line [4]. Other monohydroxylated isoflavones such as daidzein, genistein and apigenin can be converted into their corresponding dihydroxylated isoflavones such as 3'-ODI, orobol, and tricetin, having potent antioxidant properties. Such natural phytochemical compounds have great potentials as dietary supplements and therapeutic reagents owing to their cholesterol lowering effect, cardiovascular protection function, antitumor activity, anticarcinogenic properties and etc. [5-8]. However, their large scale chemical syntheses are rather difficult and very costly to be used as dietary supplements, and their

pharmacological effects as therapeutic reagents are not well elucidated often due to lack of enough materials to proceed safety and efficacy tests. To produce the above mentioned diphenolic natural phytochemicals in large quantity using tyrosinase, tyrosinase has a major drawbacks generating melanin products randomly formed from quinonic compounds, which are further oxidized from the diphenolic compounds. Such problems were also partially solved by the addition of excess inhibitor and/or antioxidant [3]. However, still the remaining issues are expanding its substrate specificity to accept target monophenolic compounds and increasing their selectivity for monophenolase reaction. To examine such issues in greater detail, here several isoflavones whose diphenolic form would be very useful for further biological study were selected and subjected to tyrosinase reaction using a tyrosinase from *Bacillus megaterium*. Their tyrosinase reaction rates were sometimes too low for the production of *o*-diphenol compounds or the diphenolase activity leading to melanin synthesis was so high that obtaining diphenolic compounds were hard.

Recently, several research groups showed great interests in thorough understanding of tyrosinase reaction mechanism and developing mutation methods to increase monophenolase ( $k_1$ )/diphenolase ( $k_2$ ) activity ratio [9-13]. Tyrosinase active site has two  $\text{Cu}^{2+}$  ions and six histidine residues, which are essential to hold the two  $\text{Cu}^{2+}$  ions, and the other amino acids surrounding the active site have great influence on determining their substrate specificities by facilitating easy access of substrate and efficient binding of the introduced substrate. Recent study of Citek *et al.* [13] showed that

using synthesized self-assembled metal-ligand core model of tyrosinase, the active site alone can hydroxylate phenolic substrates without surrounding polypeptide structures, suggesting that the surrounding amino acids are not involved in the reaction mechanism itself, but form key determinants for its substrate specificity. Such results give some insights on how we can change or improve substrate specificity of tyrosinase, and the ratios of  $k_1/k_2$  for specific substrates.

In order to screen the mutants with improved tyrosinase activity and of high ratio of  $k_1/k_2$ , accurate measurements of monophenolase and diphenolase activities are prerequisite and then simple color or UV spectrometric assay are desirable. To develop such screening methods, we found that several previous methods had some drawbacks to apply them for the tyrosinase reactions of phenolic natural compounds. Yosef *et al.* and Goldfeder *et al.* [10, 11] carried out a mutagenesis with tyrosinase from *Bacillus megaterium* based on modified screening method of Bottcher and Bornscheuer, and found mutants having 9-, 4.4-, and 2.6-fold higher  $k_1/k_2$  ratio for L-tyrosine as a substrate. However, their methods were limited for finding the better tyrosinase only for L-tyrosine, but not for other phenolic compounds, because a concentration of quinonic compounds from other phenolic compounds couldn't be measured easily. Molloy *et al.* demonstrated a mutagenesis of tyrosinase from *Ralstonia Solanacearum* for conversion of D-tyrosine into D-DOPA, and they screened the colonies releasing melanin on the plates including D-tyrosine [12]. This method is also limited because the tyrosinase from *Ralstonia Solanacearum* is the only one tyrosinase known so far

showing high  $k_1/k_2$  ratio above 1. Tyrosinases showing such  $k_1/k_2$  ratio above 1 have positive correlation between the rate of monophenolase reaction and melanin formation rate, but most tyrosinases showing  $k_1/k_2$  ratio below 1 do not have such a positive correlation. Therefore, the previous tyrosinase screening methods are not general enough for us to apply them for *ortho*-hydroxylation of other monophenol compounds. In addition, since the diphenolic products were subsequently used for diphenolase reaction, it was hard for us to measure and compare the maximum yield of diphenolic products for the mutants selected.

Here, two steps of product measurements were employed to solve the problems mentioned above. Firstly, 1mM of  $\text{FeCl}_3$  solution was added into the tyrosinase reaction mixture to make iron chelation with diphenolic products. This chelation prevented the diphenolic products from being consumed for the subsequent diphenolase reaction and the absorbance of the chelated products at 550 nm was measured to trace the changes in the concentrations of the diphenolic products. Secondly, 1mM of 3-methyl-2-benzothiazolinone hydrazone hydrochloride (MBTH) was added into the tyrosinase reaction mixture to measure their corresponding quinonic compounds for calculating kinetic constants of various substrates. MBTH made adducts with such quinonic compounds not to lose them for melanin synthesis reaction, and the absorption spectra of adducts were obtained between 400 nm and 600 nm, enabling us to calculate the initial formation rate of quinonic compounds [14, 15]. Using this direct measurement of the concentrations of diphenolic products and corresponding quinonic by-products, tyrosinase mutants having higher yield of dihydroxy

compounds from each substrates were selected and compared more accurately and simply.

## 2. Materials and Methods

### 2.1. Plasmids construction for recombinant tyrosinase and variants by mutagenesis

Genomic DNA was extracted from *Bacillus megaterium* with G-spin Genomic DNA extract kit (Intron, Korea), and this was used as a template of PCR for amplifying the gene of tyrosinase. The gene of tyrosinase was inserted into pET28ma (Novagen, USA), and His-tag was introduced at the end of tyrosinase.

For saturation mutagenesis at V218 position, NNK codon was used. Mutated plasmid was amplified by PCR using origin plasmid as a template with the primers named V218\_F and V218\_R. Likewise, the plasmid for N205A and R209A was amplified by PCR using origin plasmid as a template with the primers named N205A\_F, N205A\_R, R209A\_F, and R209A\_R. (primers used in this research are presented in Table 1) After amplification, the plasmid samples were treated with DpnI at 37°C for one hr to remove the template. These plasmids were transformed into *E. coli* DH5α by heat shock, and spread on Luria-Bertani media (LB) agar plates. Colonies on the plate were collected and their plasmids were obtained using Plasmid Prep Kit (GeneAll).



**Table 1.** Primer list.

Primer name	Sequence (5' → 3')
V218_F	GGACAGATGGGCGTTNNKCCTACTGCTCCGAAT
V218_R	ATTCGGAGCAGTAGGMNNAACGCCCATCTGTCC
N205_F	CCACAGCTTCACGCGCGCGTACACCGT
N205_R	ACGGTGTACGCGCGCGTGAAGCTGTGG
R209A_F	CACAATCGCGTACACGCGTGGGTTGGCGGACAG
R209A_R	CTGTCCGCCAACCACGCGTGTACGCGATTGTG

## 2.2. Expression of recombinant tyrosinase and variants for screening

Plasmids were transformed into *E.coli* BL21 by heat shock, and spread on plates of agar LB media. A colony on the plate was inoculated into a test tube with 3 mL of LB broth and incubating at 37°C, 200rpm for about 12 hrs. 1 mL of cell culture was transferred into a 250 mL flask with 50 mL of LB broth and incubating until optical density (OD) at 600nm reached about 0.6. For induction, isopropyl  $\beta$ -D-1-thiogalactopyranoside (IPTG) and  $\text{CuSO}_4$  were added; final concentrations of IPTG and  $\text{CuSO}_4$  were 0.2 mM and 1 mM. After induction, the cell mixtures were placed in an incubator at 18°C, 200 rpm for 20 hrs. A supernatant was removed after centrifuging at 4000 rpm for 10 min and a cell culture was washed with 50 mM phosphate buffer (25mL, pH 7.5). After another centrifuge, 50 mM Tris-HCl buffer (5mL, pH 8) was added and cell lysis was performed by sonication. A supernatant solution was collected after centrifuging at 15000 rpm for 25 min in 4°C.

For high-throughput screening saturation mutagenesis, library plasmids were transformed into *E.coli* BL21 by heat shock, and spread on plates of agar LB media. Each 92 colonies on the plate and 4 colonies of wild type was inoculated into a 96 deep-well plate with 400  $\mu\text{L}$  of LB broth and incubating at 37°C, 200 rpm for overnight. 4  $\mu\text{L}$  of cell cultures were transferred into other 96 deep-well plate with 400  $\mu\text{L}$  of LB broth and incubating until OD at 600nm reached about 0.6. 100  $\mu\text{L}$  of LB broth with IPTG and  $\text{CuSO}_4$  whose final concentrations were 0.2 mM and 1 mM was added for induction. The cell mixtures were placed in an incubator at 18°C, 200 rpm for 20

hrs. Supernatants were removed after centrifuging at 4000 rpm for 10 min and 100 $\mu$ L of lysozyme solution (25 mg lysozyme in 50 mL pH 7, 50 mM phosphate buffer) was added for cell lysis. After one hour in room temperature, supernatant solutions were collected by centrifuging at 4000 rpm for 25 min in 4 $^{\circ}$ C.

### **2.3. Screening method for substrates**

Screening was performed in a 96 micro plate. Each well contained 200  $\mu$ L of solution composed of FeCl<sub>3</sub> (1mM), supernatant containing tyrosinase variants (5 $\mu$ L), substrate (200  $\mu$ M of daidzein, resveratrol, or apigenin), and 500mM Tris-HCl buffer (pH 8.8). Absorbance at 550nm was measured every 30 sec while the reaction was progressing.

### **2.4. Purification of tyrosinase**

Purification was performed using His-tag purification. 5 mL solution of His<sub>6</sub>-tagged tyrosinase and variants were treated with Ni-NTA agarose (Qiagen), washed with 25 mM imidazole solution twice, and eluted with 250 mM imidazole solution. For diluting the concentration of imidazole to 100  $\mu$ M and condensing the concentration of tyrosinase, ultrafiltration was performed about 6~7 times. The final concentration of tyrosinase was measured by Bradford assay.

## 2.5. Characterization of tyrosinase

Standard curves of quinonic compound–MBTH adduction were obtained by measuring absorbance at 478 nm and 550 nm of each concentration of adduction. Reaction was performed in a 96 well micro plate. In the solution of reaction, concentrations of tyrosinase and their variants (V218S and V218G) were fixed at 300 nM, and MBTH was fixed at 1mM. Concentrations of substrates were changed from 1 mM to 31.25  $\mu$ M (daidzein and resveratrol), from 320  $\mu$ M to 20  $\mu$ M (piceatannol), and from 480  $\mu$ M to 30  $\mu$ M (3'-ODI). The volume of solution was 200  $\mu$ L, and absorbance at 478 nm and 550 nm of all these reactions were measured each 15 second, thus initial rate of reactions were obtained.

## 2.6. Oxidative reaction with substrates

Reaction was performed in a 5 mL solution of 500 mM Tris-HCl buffer (pH 8.8) containing 300 nM of purified tyrosinase and variants, and 200  $\mu$ M of substrate (daidzein, resveratrol, or apigenin) at 37°C, 200 rpm. 100  $\mu$ L of solution was used as a sample each time, and these samples were extracted by 10 fold volume of ethyl acetate. After removing total solvent using cold vacuum chamber, samples were resolved with methanol and analyzed by HPLC. Each product from substrates was separated using HPLC and evaporated by cold vacuum chamber. After resolving with ethyl acetate, products were converted to TMS (trimethylsilyl) derivatives by adding 3% sample volume of N,O-bis(trimethylsilyl) trifluoroacetamide (BSTFA) and analyzed by GC/MS.

## 2.7. Analytical methods

Samples at each time were analysed by a Shimadzu HPLC with an UV/Vis detector and a C<sub>18</sub> column (4.6 mm × 150 mm). Resveratrol and its product were analyzed with HPLC isocratic elution; 1 mL/min of 30% ACN/70% H<sub>2</sub>O for 15min, and the detection wavelength of 325 nm. Apigenin and its product were analyzed with HPLC gradient elution following Freire *et al.* for comparing with quercetin; using a water - formic acid mixture (99:1, v/v solvent A) and MeOH (solvent B) as the mobile phase: 0 - 3 min 40% B, 5 - 15 min 45% B, 17 - 25 min 50% B, 27 - 43 min 55% B, 45 min 40% B, 1.0 mL/min at 360 nm [16]. Also, apigenin and its product were analyzed with HPLC isocratic elution; 1mL/min of 30% ACN/70% H<sub>2</sub>O for 20 min at 274 nm. Daidzein and its product were analyzed with HPLC isocratic elution; 1mL/min of 25% ACN/70% H<sub>2</sub>O for 20 min, and the detection wavelength of 254 nm. GC/MS (ITQ1100<sup>TM</sup>-GC/MS<sup>n</sup>, Thermo Scientific, USA) using a non-polar capillary column (5% phenyl methyl siloxane capillary 30 m × 250 μm i.d., 0.25 μm film thicknesses) was used for identifying products. The analysis methods were as follows; for products from daidzein and resveratrol, a linear temperature gradient (65°C 1 min, temperature gradient of 30°C min<sup>-1</sup> to 250°C, hold for 3 min, then 5°C min<sup>-1</sup> to 280°C, and hold for 10 min), 280°C of injector temperature; for products from apigenin, a linear temperature gradient (65°C 1 min, temperature gradient of 30°C min<sup>-1</sup> to 250°C, hold for 3 min, then 5°C min<sup>-1</sup> to 300°C, and hold for 10 min), 300°C of injector temperature. Mass scan range was 50-600 m/z and 50-800 m/z and mass spectrum was

obtained by electron impact ionization at 70 eV. MS/MS was used for the identification of product from daidzein and apigenin.

## 3. Results and Discussion

### 3.1. Developing a screening method with substrates

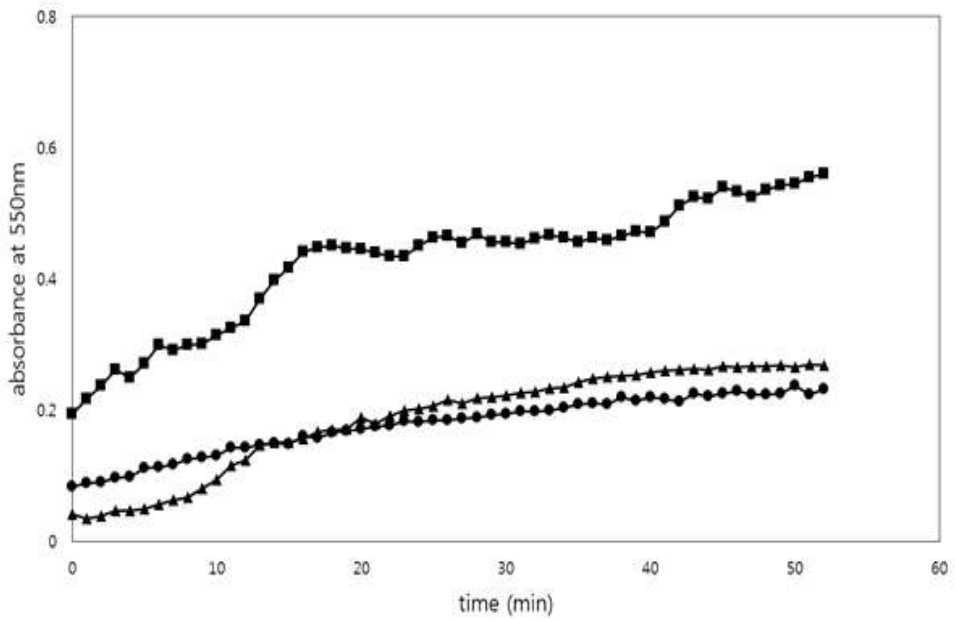
According to the mechanism of tyrosinase, tyrosinase has three forms, oxy-tyrosinase (o-tyr), met-tyrosinase (m-tyr), and deoxy-tyrosinase (d-tyr). Monophenol compounds react with o-tyr, and they are converted to diphenol compounds and m-tyr. M-tyr reacts with diphenol compounds, and produces quinonic compounds changing itself as d-tyr. D-tyr is converted to o-tyr when oxygen is added. Therefore, tyrosinase has a cyclic reaction, and the concentration of diphenol compounds, intermediates of total reaction, is increased at first but decreased after passing the maximal concentration. We assumed that the maximal concentration of diphenol compounds is related with the ratio of  $k_1$  to  $k_2$  because these two kinetic constants dominate the concentration of diphenol compounds.

The previous screening method was measuring the maximal concentration of diphenol compounds. By ceasing the reaction when diphenol compounds' concentration was maximum using high concentration of iron, each mutants was screened by bare eye. These procedure had a critical flaws. First, each mutant had different time point when the concentration of diphenol compounds is maximum because they had different ratio of  $k_1$  to  $k_2$ . Thus, stopping all libraries at the same time couldn't measure the maximal concentration

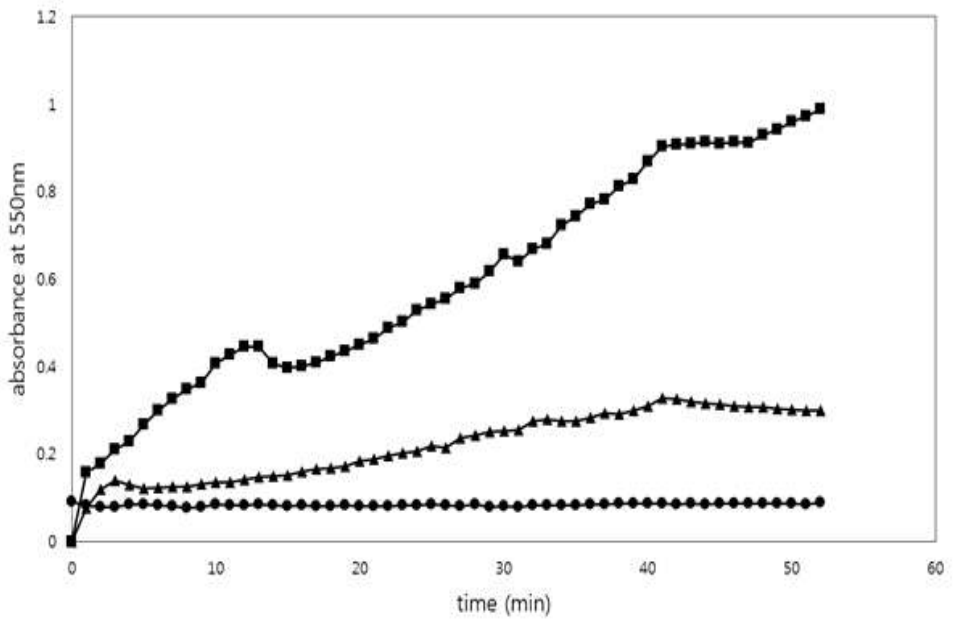
of diphenol compounds. Secondly, screening with bare eye was inaccurate and strenuous. The color of iron chelation was mixed with the color of melanin and this made hard to screen. Therefore, obtaining quite accurate diphenol compounds' concentration in real time was required.

For tracing the concentration of diphenol compounds, 1 mM of  $\text{Fe}^{3+}$  was added to tyrosinase reaction for forming complex with diphenol compounds showing absorption spectra at 550 nm and 500 mM of pH 8.8 Tris-HCl buffer was used for preventing the change of pH [14]. We confirmed that the absorbance of melanin at 550 nm in the condition of screening is low enough to ignore and the correlation exists between the concentration and the absorbance of complex. (Figure 1) The schematic diagram of screening is shown in Figure 2.

(a)

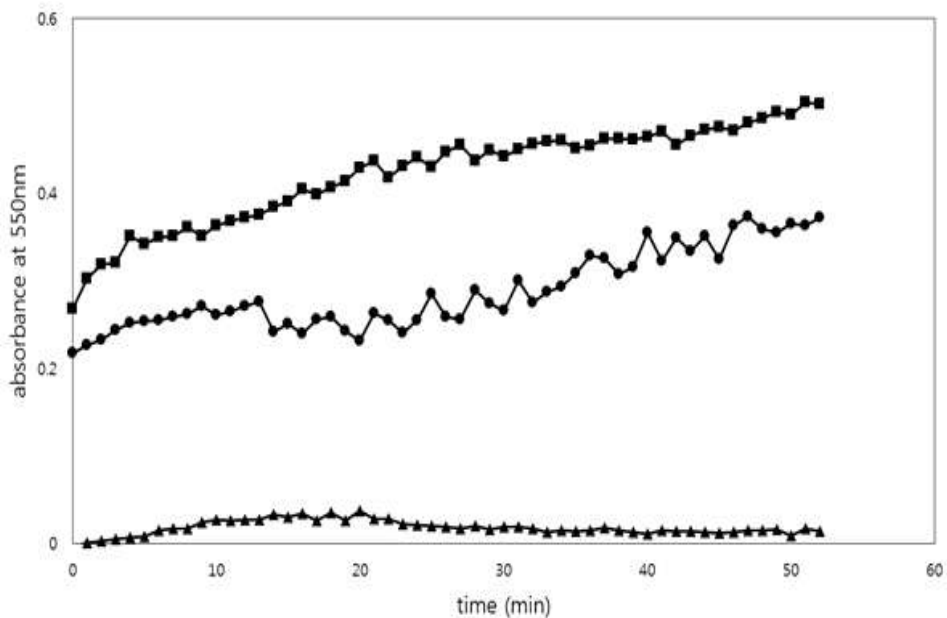


(b)





(c)



(d)

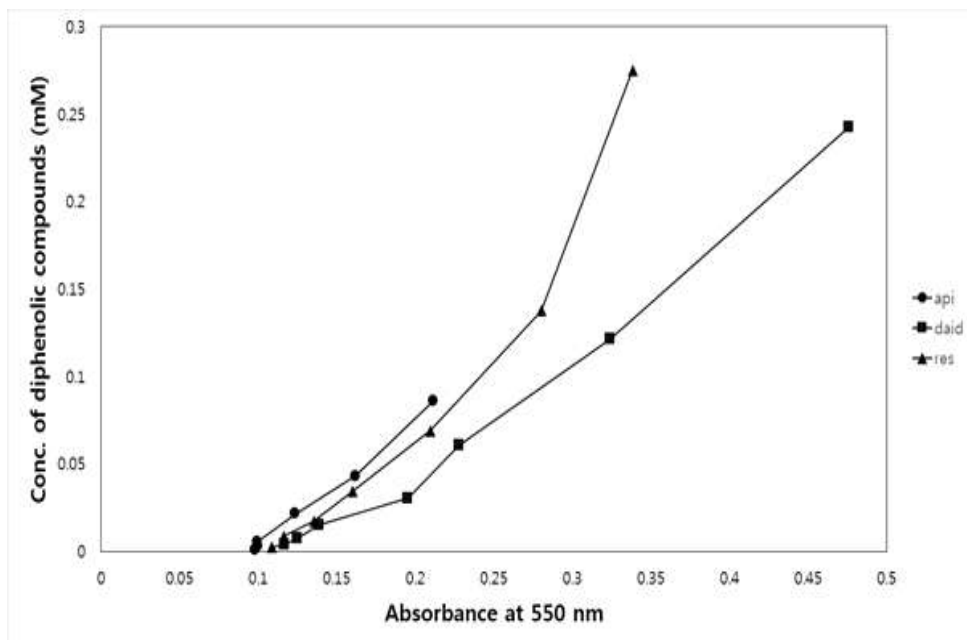
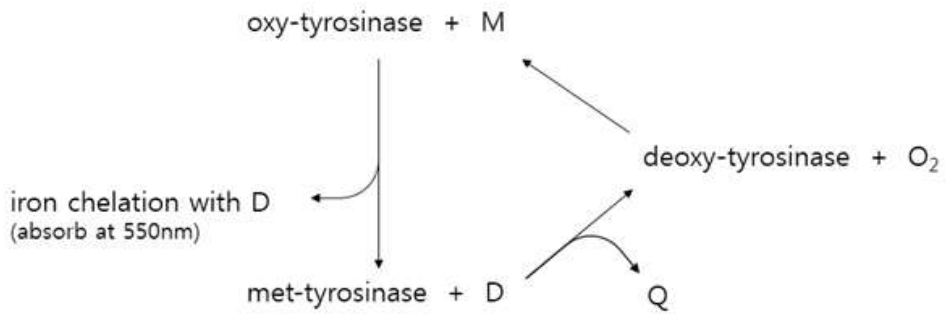
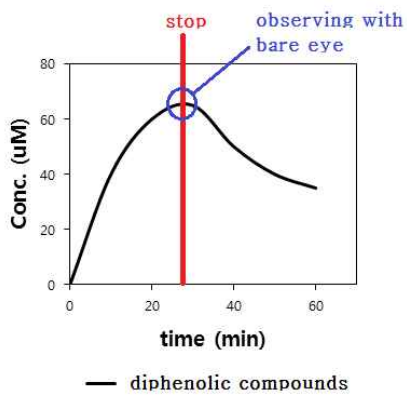


**Figure 1.** Absorbance at 550 nm of reaction with various conditions for testing screening method. (a) Reaction with tyrosinase, 200  $\mu\text{M}$  of daidzein and 1 mM of  $\text{FeCl}_3$  (square), reaction with 200  $\mu\text{M}$  of daidzein and 1 mM of  $\text{FeCl}_3$  (round), reaction with tyrosinase and 200  $\mu\text{M}$  of daidzein (triangle). (b) Reaction with tyrosinase, 200  $\mu\text{M}$  of resveratrol and 1 mM of  $\text{FeCl}_3$  (square), reaction with 200  $\mu\text{M}$  of resveratrol and 1 mM of  $\text{FeCl}_3$  (round), reaction with tyrosinase and 200  $\mu\text{M}$  of resveratrol (triangle). (c) Reaction with tyrosinase, 200  $\mu\text{M}$  of apigenin and 1 mM of  $\text{FeCl}_3$  (square), reaction with 200  $\mu\text{M}$  of apigenin and 1 mM of  $\text{FeCl}_3$  (round), reaction with tyrosinase and 200  $\mu\text{M}$  of apigenin (triangle). (d) Relation between a concentration of diphenolic compounds and an absorbance.

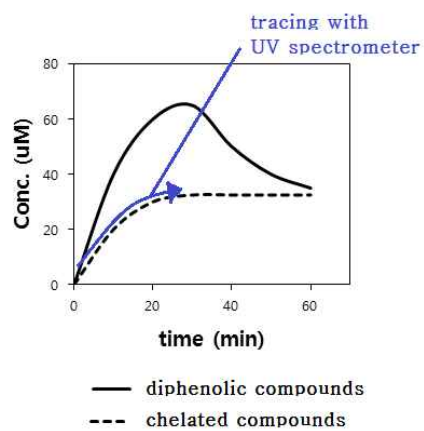
(a)



(b)



<Previous screening method>



<Improved screening method>

**Figure 2.** (a) Strategy of screening method based on the cycle of tyrosinase. (b) Comparison with previous screening method and improved screening method.

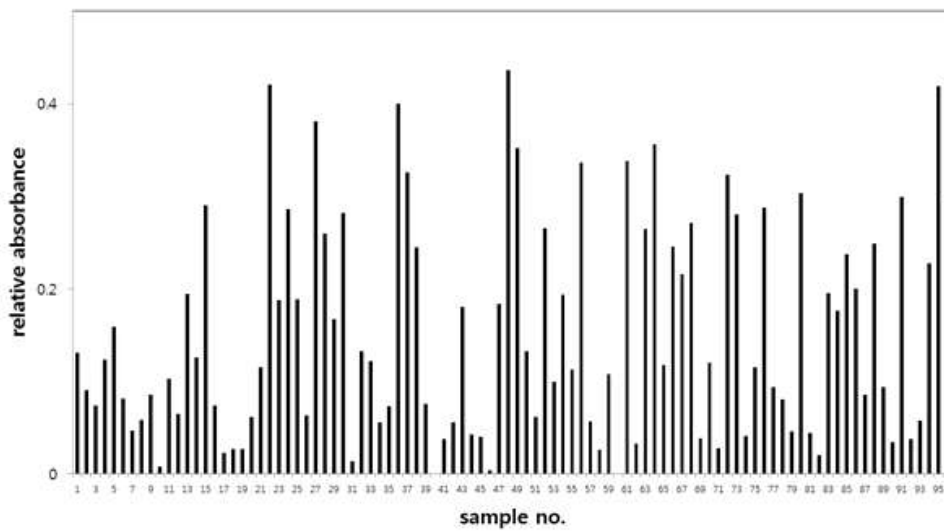
### 3.2. Selecting residues for mutagenesis and screening for high yield of substrates

Tyrosinase from *Bacillus megaterium* was selected for the *ortho*-hydroxylation of daidzein, resveratrol, and apigenin, since its previous mutation study was available in public. Yosef et al. and Goldfeder et al. [10, 11] used the same *B.megaterium* tyrosinase and mutations for the oxidation of tyrosine was investigated. To enhance the ratio of monophenolase ( $k_1$ )/ diphenolase ( $k_2$ ) activity, they identified V218 and R209. V218 is located on the loop nearby CuA and the mutant V218F substituting phenylalanine for valine improved the ratio of  $k_1/k_2$ . They proposed that the flexibility of phenylalanine proved by crystal structures affects the monophenolase activity. R209 is located nearby CuB and the mutant R209H substituting histidine for arginine improved the ratio of  $k_1/k_2$  because the imidazole ring of histidine obstructs the entrance to the active site and interferes with L-DOPA binding to CuB. When *B.Megaterium* tyrosinase goes to the three substrates mentioned above, V218 is also located in the entrance region and becomes the nearest residue with the CuA except the six histidines located in the active site. Other residues located in the entrance region nearby CuB may change the ratio of  $k_1/k_2$ , but the possibility seems low because the entrance region nearby CuB is complicated with many other residues. In result, a saturation mutagenesis at V218 site was executed and screened with daidzein, resveratrol, and apigenin as substrates. After screening V218 library with apigenin ,we couldn't find better mutants than wildtype. So, we simulated a tyrosinase-apigenin docking by autodock program. We suggested that the interaction between a carbonyl group and oxygen

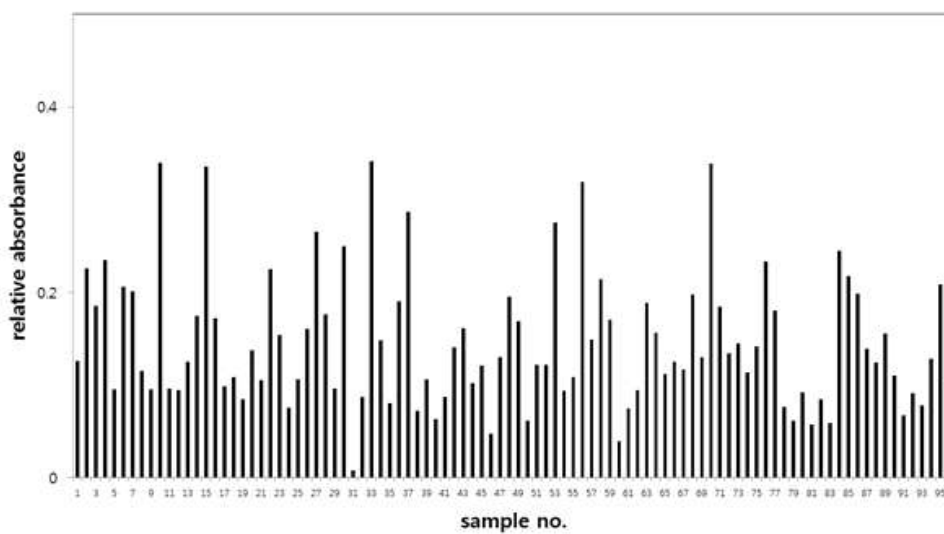
on the C-ring of apigenin and the amine group of R209 and N205 interrupted the proper position of apigenin in the active site so we changed R209 and N205 to alanine.

Using the above screening method based on the changes in UV absorbance at 550 nm while the reaction is in progress with 1mM of FeCl<sub>3</sub>, 12 and 5 variants were selected with daidzein and resveratrol. (Figure 3) In the case of daidzein, the three among five variants had V218S mutation, and the rest two mutants had an alanine or threonine exchanges. V218S produced 1.25 fold higher 3'-ODI (55µM) yield than wild type in the 5mL reaction with 200µM daidzein. (Figure 4) In the case of resveratrol, 8 of 12 variants had V218G mutation, and the rests had a leucine, isoleucine, threonine, or serine exchanges, respectively. V218G mutant produced 4.4 fold higher piceatannol (20µM) than wild type in the 5mL reaction with 200µM resveratrol. (Figure 4) For screening the mutants for apigenin, we couldn't find any mutants better than wild type in V218 library. (Figure 3) Based on the crystal structure of tyrosinase, modeling, and autodock program mentioned above, we screened R209A, N205A, and N205A/R209A (double mutant) with apigenin as a substrate. Only R209A showed better yield than wild type. (Figure 3) R209A mutant produced 1.35 fold higher tricetin (15µM) than wild type in the 5mL reaction with 200µM apigenin. (Figure 4) All the reaction products were measured by HPLC.

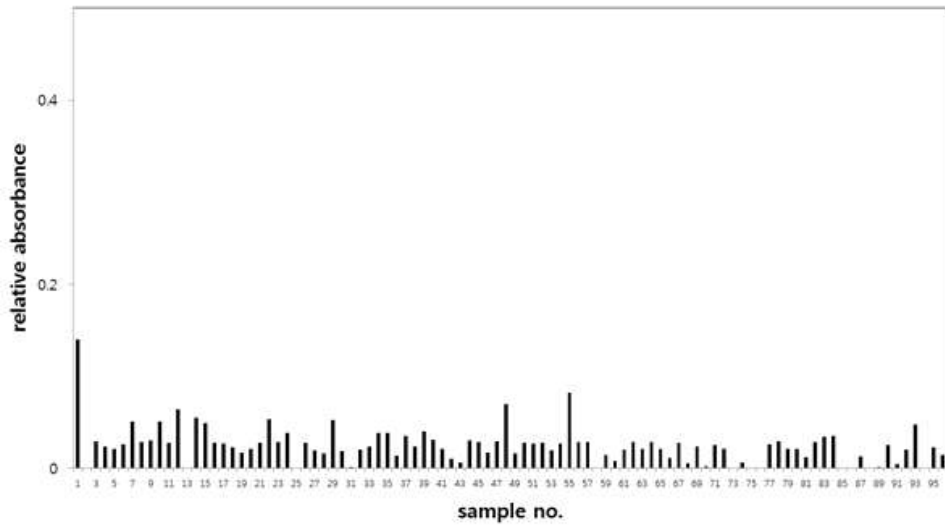
(a)



(b)



(c)



(d)

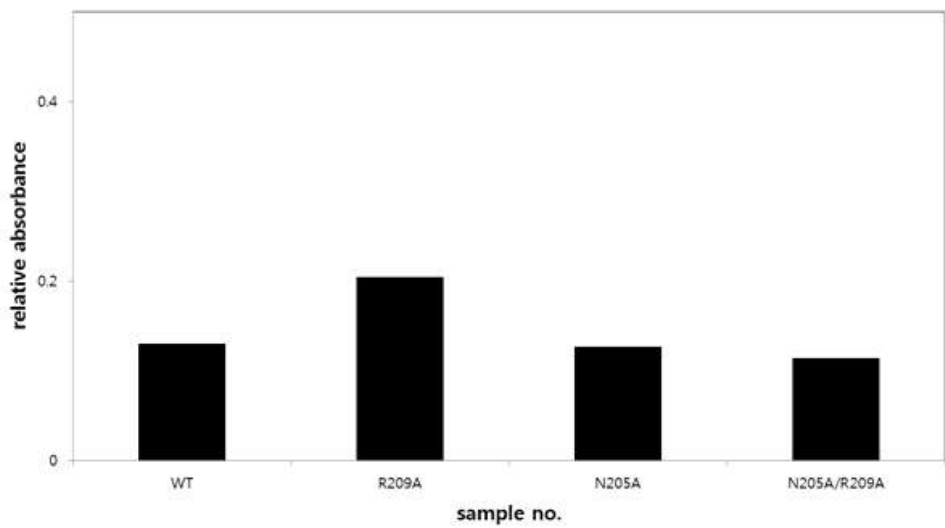
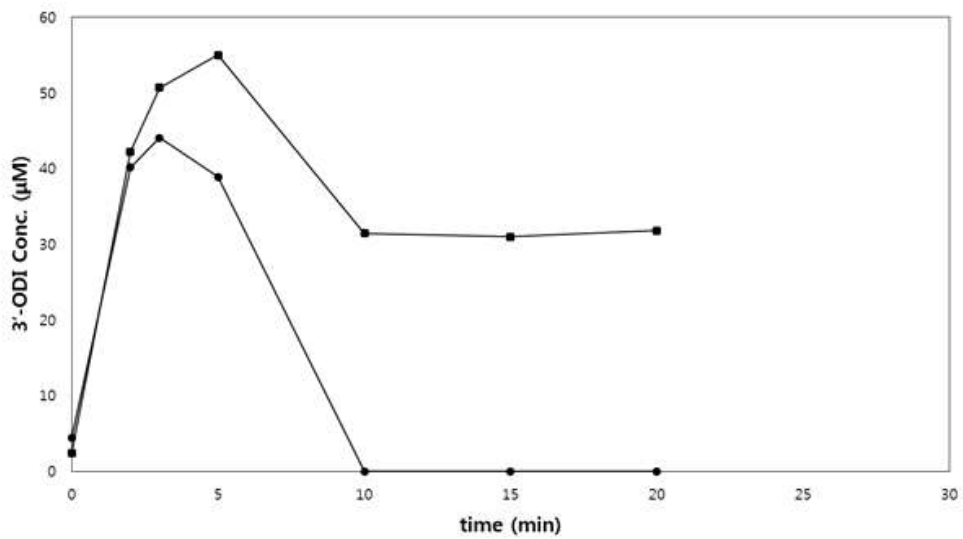


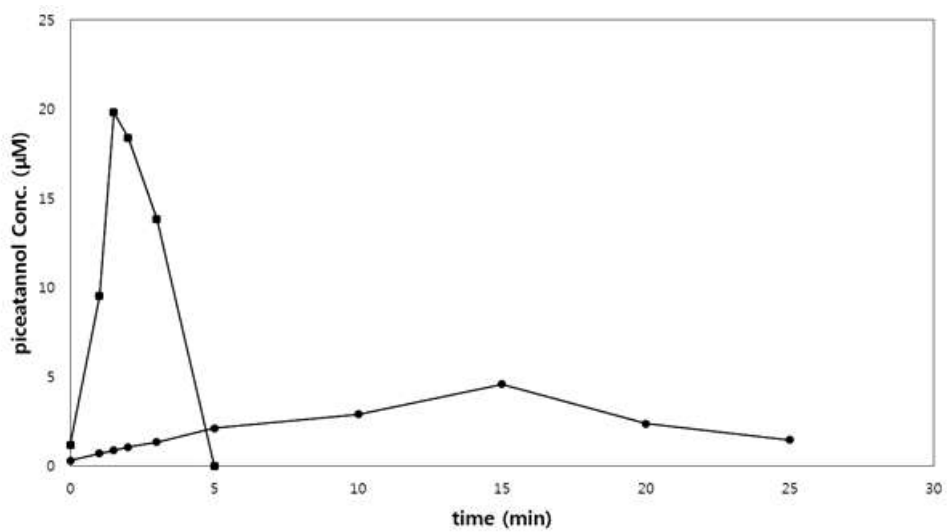


**Figure 3.** Result of screening by phenolic natural compounds with libraries. (a) Result of screening by daidzein with V218 library. (b) Result of screening by resveratrol with V218 library. (c) Result of screening by apigenin with V218 library. (d) Result of screening by apigenin with R209A, N205A, and N205A/R209A. Relative absorbance was obtained by subtracting value of initial point of reaction with mutants from value of end point of reaction with mutants. All 96 samples' absorbance at 550 nm was measured by UV spectrometer every 30 sec. Wild type was sample 1, 35, 55, 88.

(a)



(b)



(c)

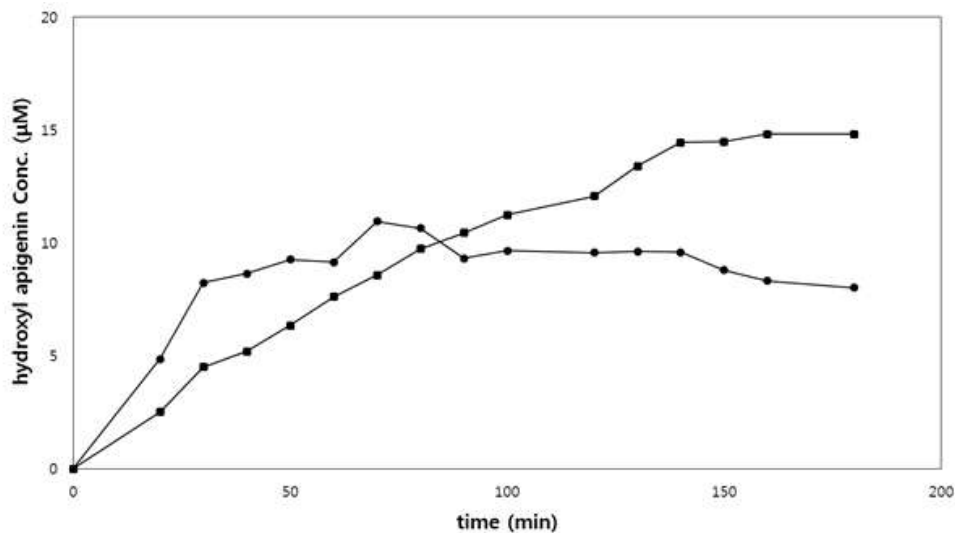
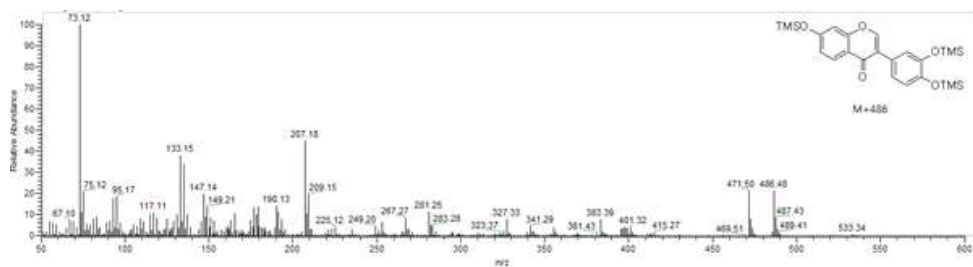


**Figure 4.** (a) 3'-ODI concentration of reaction with wild type and V218S. Square is the reaction with V218S and round is the reaction with wild type. (b) Piceatannol concentration of reaction with wild type and V218G. Square is the reaction with V218G and round is the reaction with wild type. (c) Tricetin concentration of reaction with wild type and R209A. Square is the reaction with R209A and round is the reaction with wild type. Reaction was performed with 200 µM of substrates and 300 nM of tyrosinase in 5 mL, 500 mM of Tris-HCl buffer (pH 8.8).

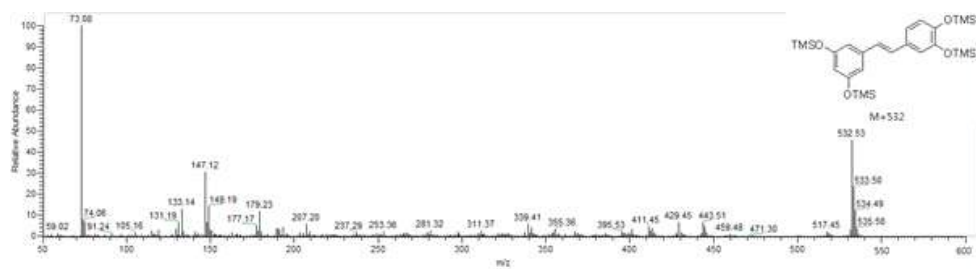
### 3.3. Identification of products from each substrate

Products were analyzed by GC/MS and GC/MS/MS after trimethylsilylation with BSTFA. The product peaks of daidzein (retention time = 18.18 min) were 3'-ODI (3 TMS) ( $m/z = 486.48$ ), and a loss of methyl group from the TMS ether moiety of 3'-ODI ( $m/z = 471.50$ ). (Figure 5.(a)) Peaks of  $m/z = 253.43, 383.55, 399.59$  in the result of GC/MS/MS also showed that the product is 3'-ODI. (Figure 5.(d)) Similarly, the peaks of piceatannol (retention time = 14.82 min) were shown at  $m/z = 532.53$  and  $517.45$ . (Figure 5.(b)) Meanwhile, the peaks of the product from apigenin (retention time = 23.90 min) were  $m/z = 662.77$  and  $647.84$ , suggesting that hydroxylation took place at two sites because of 176 (2 of -OTMS) mass increase from that of apigenin. (Figure 5.(c)) According to the result of GC/MS/MS and HPLC result that the method from Freire *et al.* was used [16] (Figure 5.(e) and Figure 6), we found that only B-ring of apigenin is hydroxylated twice and the product is tricetin.

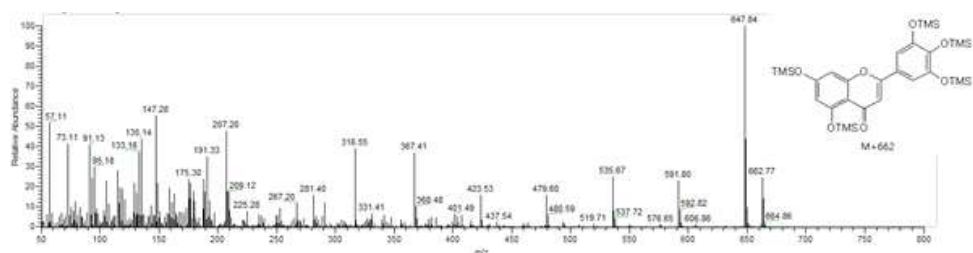
(a)



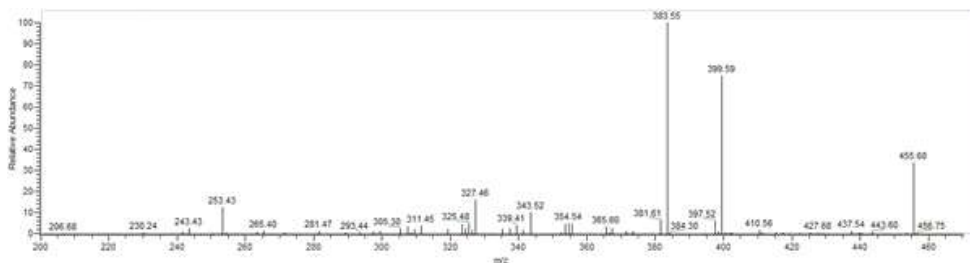
(b)



(c)



(d)



(e)

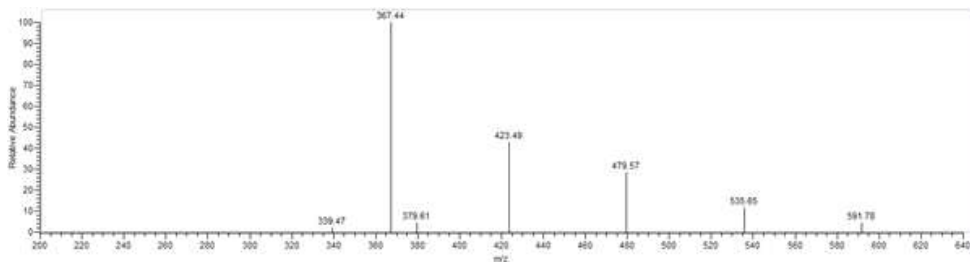
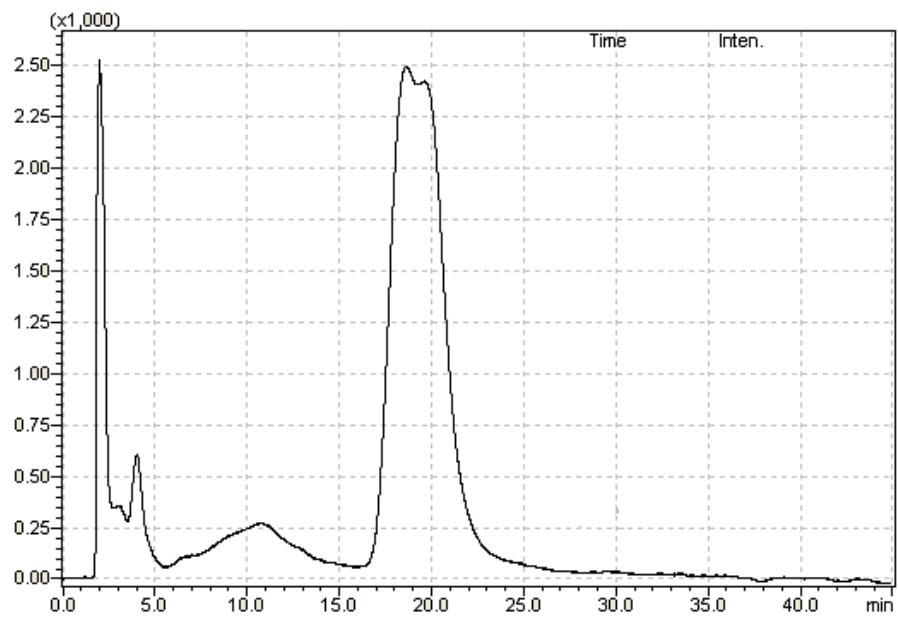


**Figure 5.** Representative GC/MS electron impact mass spectra of TMS derivatives of products. (a) Product from daidzein. (b) Product from resveratrol. (c) Product from apigenin. Representative GC/MS/MS electron impact mass spectra of TMS derivatives of (d) product from daidzein ( $m/z = 471$ ) and (e) product from apigenin ( $m/z = 647$ )

(a)



(b)

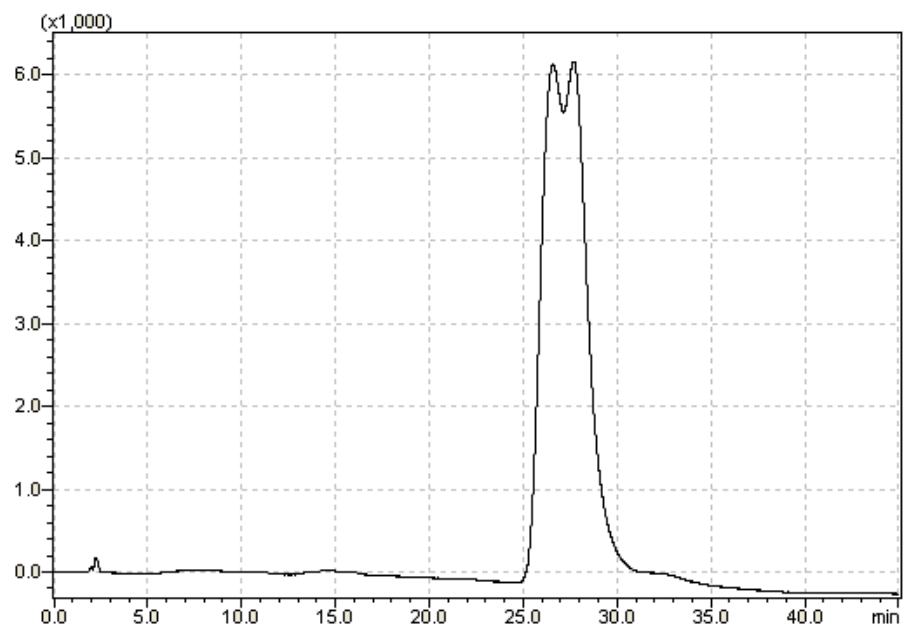


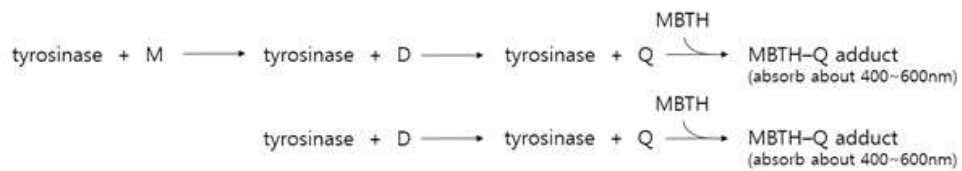
**Figure 6.** HPLC data of (a) product from apigenin and (b) quercetin. Method from Freire *et al.* was used for analysis. According to the result of GC/MS/MS of product from apigenin (Figure 5. (e)), hydroxylation took place at B-ring or C-ring of isoflavonoid. Since this data showed that the product from apigenin isn't same with quercetin, it is proved that hydroxylation took place at B-ring twice.



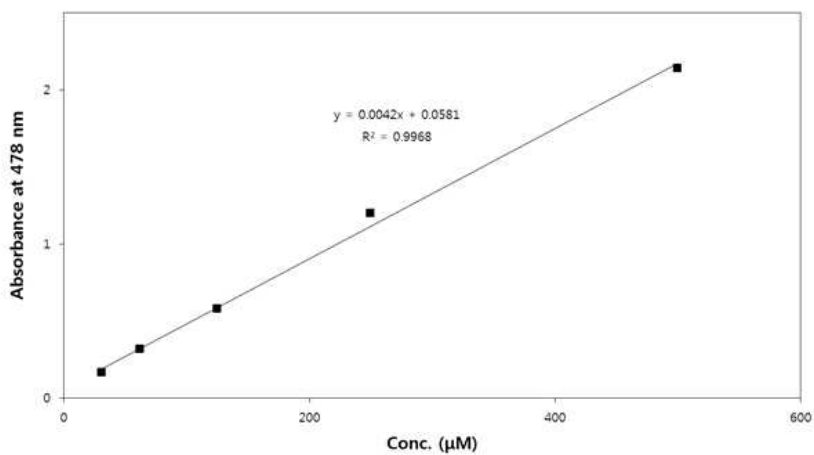
### 3.4. Developing a method for measuring kinetic constants

For developing a method of measuring kinetic constants, we modified the method from Goldfeder *et al.* which obtains an initial reaction rate from measuring the concentration of dopachrome from reactions using L-tyrosine and L-DOPA as a substrate. MBTH adduct was used for measuring the concentration of quinonic compounds from daidzein and resveratrol. MBTH was known for making adduct with quinonic compounds, and these adducts prevent quinonic compounds from forming melanin. The concentration of adducts can be obtained by measuring the absorbance at 550 nm for quinonic compound from daidzein and 478 nm for quinonic compounds from resveratrol. A standard curve of an absorbance of MBTH-quinonic compounds adduct versus concentration of quinonic compounds (from daidzein and resveratrol) was drawn and confirmed that it had a linear correlation. (Figure 7. (b), (c)) Using a standard curve, we measured the change of concentration of quinonic compounds from reactions with daidzein and resveratrol (for measuring initial reaction rate of  $v_{\text{mono}}$ ), and 3'-ODI and piceatannol (for measuring initial reaction rate of  $v_{\text{di}}$ ) as substrates. The initial reaction rates and kinetic constants were calculated by this data. Figure 7.(a) represents the scheme of obtaining kinetic constants.

(a)



(b)



(c)

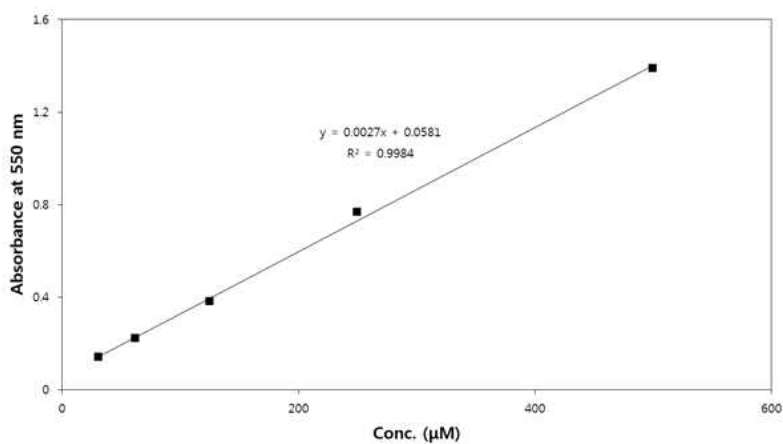


**Figure 7.** (a) The scheme for obtaining kinetic constants of tyrosinase with phenolic natural compounds. (b) Relation between the MBTH-quinonic compounds from daidzein and an absorbance. (c) Relation between the MBTH-quinonic compounds from resveratrol and an absorbance.

### 3.5. Characterization of mutants and interpretation with modeling and docking

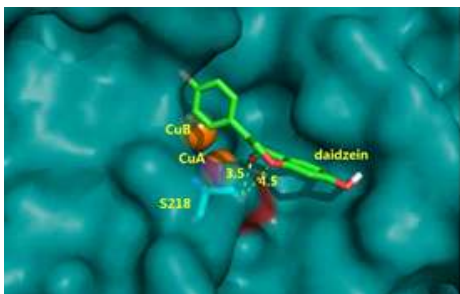
As the next step, the kinetic parameters of the mutants were measured using the absorbance of quinonic compound–MBTH adduct. (Table 2) Comparing wild type and V218S's kinetic constants of daidzein,  $V_{\max}$  of mono-phenolase of V218S was decreased about half than wildtype, but the ratio of  $V_{\max}$  ( $V_{\max\text{mono}}/V_{\max\text{di}}$ ) was increased about 10.7 fold and bigger than 1. Because of these kinetic constants, V218S produced more 3'-ODI (1.3 fold) and this 3'-ODI decreased very slowly. Comparing wild type and V218G's kinetic constants of resveratrol,  $V_{\max}$  of mono-anddi-phenolase of V218G was increased about twice of wild type, and the ratio of  $V_{\max}$  was also increased about 1.38 fold than wild type. Therefore, the reaction rate of V218G was faster and the yield of piceatannol was higher than wild type (4.4 fold).

According to the homology model of mutants derived from the crystal structure of tyrosinase from *Bacillus megaterium* (PDB: 3NM8), the oxygen and carbonyl group on the C-ring of isoflavonoid (daidzein and 3'-ODI) are likely to interact with hydroxyl group of serine in V218S mutant. Using autodock simulation, when daidzein or 3'-ODI docked in the active site properly, the distance between oxygen and carbonyl group of isoflavonoid and hydroxyl group of serine was about 6–10Å. However, in result of inappropriate pose, this distance was about 3–5Å which is near enough to interact. (Figure 8.(a), (b), (c), (d)) We suggested that this interaction between daidzein, 3'-ODI and serine residue interferes substrates approaching the active site and has an effect on kinetic constants. Since the

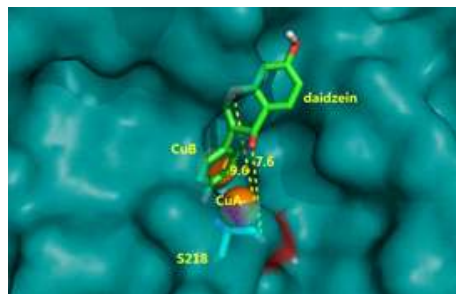
decrease of  $V_{\max}$  of 3'-ODI between wild type and V218S was much larger than decrease of  $V_{\max}$  of daidzein (about 9 fold), it was supposed that the interaction between 3'-ODI and serine is stronger than the interaction between daidzein and serine when substrates approach to the active site.

In the case of V218G mutant, the entrance of V218G for resveratrol and piceatannol appeared to be larger than that of the wild type, [10] which allowed resveratrol to access active site easily, and resulting higher reaction rate than wild type. When the surface above CuA and CuB are compared, CuA of V218G mutant has more widely opened surface than CuB of V218G. (Figure 8.(e) and (f)) It is more likely that this asymmetric increase in the exposed surface above CuA ion would result the high ratio of monophenolase to diphenolase activity of resveratrol, yielding high productivity of piceatannol.

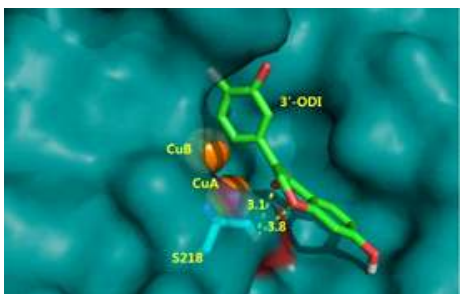
(a)



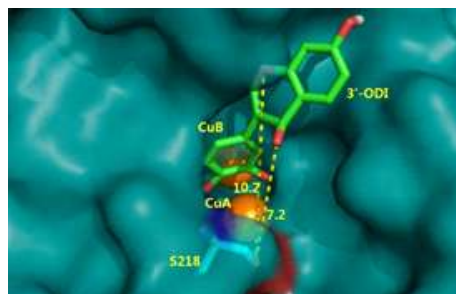
(b)



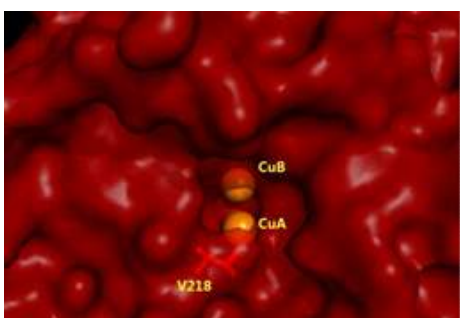
(c)



(d)



(e)



(f)

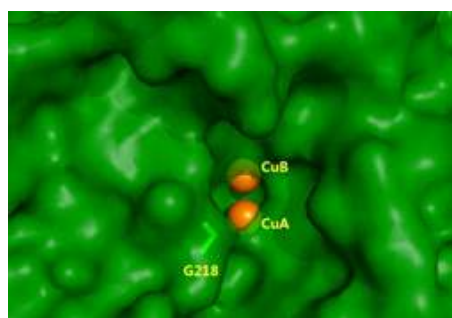


**Figure 8.** Crystal structure and homology models of wild type, V218S, and V218G. The result of docking simulation of V218S and daidzein, 3'-ODI. Each model has two Cu (orange spheres). (a) Docking simulation of V218S and daidzein, the inappropriate position. Green structure is daidzein. Cyan structure is S218 and the red part is oxygen of S218. (b) Docking simulation of V218S and daidzein, the proper position. (c) The inappropriate position of docking simulation of V218S and 3'-ODI. (d) The proper position of docking simulation of V218S and 3'-ODI. (e) Crystal structure of wild type. Red structure is V218. (f) Homology model of V218G. Green structure is G218.

**Table 2.** Kinetic constants of wild type, V218S, and V218G with phenolic natural compounds

		$V_{\max}$	$k_{\text{cat}}/K_m$	$V_{\max\text{mono}}/V_{\max\text{di}}$
		(mM/min)	( $\text{min}^{-1}\text{mM}^{-1}$ )	
Wild type	Resveratrol	0.0016	69.0	0.5
	Piceatannol	0.0032	34.6	
	Daidzein	0.0094	941.8	0.82
	3'-ODI	0.0098	257.5	
V218S	Daidzein	0.0090	456.9	8.74
	3'-ODI	0.00103	144.9	
V218G	Resveratrol	0.0038	10.3	0.69
	Piceatannol	0.0055	204.9	



## 4. Conclusion

In this study, we developed a screening method for finding tyrosinase variants which have improved yield of 3'-ODI, piceatannol, or tricetin. Combining rational site-directed saturation mutagenesis with tyrosinase from *Bacillus megaterium* and our high-throughput screening method, three variants, i.e. V218S, R209A, and V218G were selected. Compared to its wild type *Bacillus megaterium* tyrosinase, V218S, V218G, and R209A mutants showed 1.3 fold higher yield of 3'-ODI, 4.4 fold higher yield of piceatannol, and 1.35 fold higher yield of tricetin, respectively. After measuring  $k_1/k_2$  ratio using MBTH, we found that V218S had 10.7 fold  $k_1/k_2$  ratio for daidzein and V218G had 1.38 fold  $k_1/k_2$  ratio for resveratrol.

## References

1. H. Decker, R. Dillinger, F. Tuczek, How does tyrosinase work? Recent insights from model chemistry and structural biology, (2000) *Angew. Chem. Int. Ed.*, 39, pp. 1587 - 1591
2. Greta Faccio, Kristiina Kruus, Markku Saloheimo, Linda Thöny-Meyer, Bacterial tyrosinases and their applications, (2013) *Process Biochemistry*, Vol 47, Issue 12, pp 1749-1760
3. Nahum Lee, Eun Jung Kim, and Byung-Gee Kim, Regioselective Hydroxylation of trans-Resveratrol via Inhibition of Tyrosinase from *Streptomyces avermitilis* MA4680, (2012) *ACS Chem, Biol.*, Vol 7, Issue 10, pp 1687-1692
4. Wieder T, Prokop A, Bagci B, Essmann F, Bernicke D, Schulze-Osthoff K, Dörken B, Schmalz HG, Daniel PT, Henze G, Piceatannol, a hydroxylated analog of the chemopreventive agent resveratrol, is a potent inducer of apoptosis in the lymphoma cell line BJAB and in primary, leukemic lymphoblasts., (2001) *Leukemia*, Vol 15, Issue 11, pp 1735-1742
5. Stanley Z. Dziedzic, Bertram J.F. Hudson, Hydroxy isoflavones as antioxidants for edible oils, (1983) *Food Chemistry*, Vol 11, Issue 3, pp 161-166
6. Kang NJ, Lee KW, Rogozin EA, Cho YY, Heo YS, Bode AM, Lee HJ, Dong Z., Equol, a metabolite of the soybean isoflavone daidzein,

inhibits neoplastic cell transformation by targeting the MEK/ERK/p90RSK/ activator protein-pathway. *J Biol Chem*, Vol 282, pp 32856 - 32866.

7. Rüfer CE, Kulling SE., Antioxidant activity of isoflavones and their major metabolites using different in vitro assays., (2006), *J Agric Food Chem*, Vol 54, pp 2926 - 2931

8. C Rice-Evans, N Miller, G Paganga, Antioxidant properties of phenolic compounds, (1997), *Trends in Plant Science*, Vol 2, Issue 4, pp 152-159

9. Jose Luis Muñoz-Muñoz, Jose Berna, María del Mar García-Molina, Francisco Garcia-Molina, Pedro Antonio Garcia-Ruiz, Ramon Varon, Jose N. Rodriguez-Lopez, Francisco Garcia-Canovas, Hydroxylation of p-substituted phenols by tyrosinase: Further insight into the mechanism of tyrosinase activity, (2005), *J. Am. Chem. Soc.*, Vol 127, Issue 51, pp 18031-18036

10. Mor Goldfeder, Margarita Kanteev, Noam Adir, Ayelet Fishman, Influencing the monophenolase/diphenolase activity ratio in tyrosinase, (2013), *Biochimica et Biophysica Acta*, Vol 1834, Issue 3, pp 629-633

11. Vered Shuster Ben-Yosef, Mor Sendovski, Ayelet Fishman, Directed evolution of tyrosinase for enhanced monophenolase/diphenolase activity ratio, (2010), *Enzyme and Microbial Technology*, Vol 47, pp 372-376

12. Susan Molloy, Jasmina Nikodinovic-Runic, Leona B. Martin, Hermann Hartmann, Francisco Solano, Heinz Decker, Kevin E. O'Connor, Engineering of a bacterial tyrosinase for improved catalytic efficiency towards D-tyrosine using random and site directed mutagenesis approaches, (2013), *Biotechnology and Bioengineering*, Vol 110, Issue 7, pp 1849-1857
13. Cooper Citek, Christopher T. Lyons, Erik C. Wasinger & T. Daniel P. Stack, Self-assembly of the oxy-tyrosinase core and the fundamental components of phenolic hydroxylation, (2012) *Nature Chemistry*, Vol 4, pp 317-322
14. Mirjana Andjelković, John Van Camp, Bruno De Meulenaer, Griet Depaemelaere, Carmen Socaciu, Marc Verloo, Roland Verhe, Iron-chelation properties of phenolic acids bearing catechol and galloyl groups, (2006), *Food Chemistry*, Vol 98, Issue 1, pp 23-31
15. Alison J. WINDER, Henry HARRIS, New assays for the tyrosine hydroxylase and dopa oxidase activities of tyrosinase, (1991), *European Journal of Biochemistry*, Vol 198, Issue 2, pp 317-326
16. Kristerson R.L. Freire, Antonio C. S. Lins, Marcos C. Dórea, Francisco A. R. Santos, Celso A. Camara and Tania M. S. Silva, Palynological Origin, Phenolic content, and Antioxidant Properties of Honeybee-collected Pollen from Bahia, Brazil, (2012), *Molecules*, Vol 17, pp 1652-1664

## 국문 초록

타이로시나아제를 이용한 다이드제인, 레스베라트롤, 아피제닌의 오르토-모노하이드록실화에 대한 연구가 최근 많이 진행되고 있다. 타이로시나아제는 모노페놀 물질을 다이페놀 물질로 하이드록실화하는 첫 번째 반응과 다이페놀물질을 퀴논형 물질로 산화시키는 두 번째 반응을 연속적으로 일으킨다. 두 번째 반응인 산화 반응이 첫 번째 반응의 산물인 다이페놀 물질을 소모하기 때문에 다이페놀 물질에 대한 생산 수율은 상당히 낮고, 이에 따라 타이로시나아제를 이용한 모노하이드록실화 반응은 한계점을 가지고 있다. 이러한 한계점을 극복하기 위해서 타이로시나아제의 첫 번째 반응의 활성 ( $k_1$ )과 두 번째 반응의 활성 ( $k_2$ )에 대한 비율을 조절하는 연구가 진행되어 왔다.

$k_1$  과  $k_2$  의 비율을 조절하기 위하여 우리는 스크리닝 방법과 반응속도상수를 계산할 방법을 개발하였고 *Streptomyces avermitilis* MA4680 유래의 타이로시나아제 (SAV1137)에 대해 포화 돌연변이 기법을 수행하고 스크리닝을 진행하였다. 결과적으로 1.4 배의 수율과 1.4 배의  $k_1$  과  $k_2$  의 비율을 가지는 하나의 돌연변이 단백질을 찾았으나 이를 찾기 위한 과정은 굉장히 힘들었고 정확도가 상당히 저조하였다. 스크리닝 방법을 통하여 300 종류의 변이 단백질 중 5개의 변이 단백질을 찾았으나 그 중 한 개만이 의미있는 값을 보였고 나머지 단백질들은 오히려 감소한 값을 보였다. 따라서, 정확도가 개량되고 용이한 스크리닝 방법이 요구되었다.

버퍼 용액의 세기와 수소이온지수, 철과 효소용액의 농도, 그리고 3-methyl-2-benzothiazolinone hydrazone hydrochloride (MBTH)를 첨가하는 방법을 통하여 다이페놀 물질의 농도에 대한 상대적인 값을 실

시간으로 추적할 수 있는 스크리닝 방법과 변이 단백질에 대한 반응속도 상수를 정확하게 구할 수 있는 방법을 개발하였다.

개선된 스크리닝 방법을 시험해보기 위하여 *Bacillus megaterium* 유래의 타이로시나아제에 대한 x 선 결정구조와 homology model, docking 시뮬레이션을 기반으로 포화 돌연변이 기법을 수행하였다. 그 결과, 세 가지 기질에 대해서 생산수율과  $k_1$  과  $k_2$  의 비율이 증가한 각각 변이 단백질을 스크리닝 기법을 통하여 찾을 수 있었다. V218S 는 7,3',4'-trihydroxyisoflavone (3'-ODI) 생산수율이 30%, V218G 는 피세타놀 생산수율이 440%, 그리고 R209A 는 트리세틴 생산수율이 40%가 증가하는 것을 확인하였다. 또한, V218S 는  $k_1$  과  $k_2$  의 비율이 10.7 배, V218G 는 1.4 배 증가한 것을 확인할 수 있었다.

**주요어** : 타이로시나아제, 스크리닝, *Bacillus megaterium*, 철 킬레이션, 다이드제인, 레스베라트롤

**학번** : 2012-20950